Enthalpy−Entropy Contributions to the Potential of Mean Force of Nanoscopic Hydrophobic Solutes

Niharendu Choudhury† and B. Montgomery Pettitt*

Department of Chemistry, University of Houston, Houston, Texas 77204-5003

Received: November 28, 2005; In Final Form: February 9, 2006

Entropic and enthalpic contributions to the hydrophobic interaction between nanoscopic hydrophobic solutes, modeled as graphene plates in water, have been calculated using molecular dynamics simulations in the isothermal−isobaric (NPT) ensemble with free energy perturbation methodology. We find the stabilizing contribution to the free energy of association (contact pair formation) to be the favorable entropic part, the enthalpic contribution being highly unfavorable. The desolvation barrier is dominated by the unfavorable enthalpic contribution, despite a fairly large favorable entropic compensation. The enthalpic contributions, incorporating the Lennard-Jones solute−solvent terms, largely determine the stability of the solvent separated configuration. We decompose the enthalpy into a direct solute−solute term, the solute−solvent interactions, and the remainder that contains pressure−volume work as well as contributions due to solvent reorganization. The enthalpic contribution due to changes in water−water interactions arising from solvent reorganization around the solute molecules is shown to have major contribution in the solvent induced enthalpy change.

I. Introduction

The hydrophobic interaction (HI) causes[1−4] a nonpolar solute dissolved in water to display various forms of aggregation, organization, and self-assembly.[5] It is generally believed that manifestations of hydrophobicity are length scale dependent. Therefore, a complete understanding of hydrophobicity remains elusive.

Water is a network forming liquid due to extensive hydrogen bonding between the molecules. Due to lack of hydrogen bonding between water and hydrophobic units, dissolution of a hydrophobic solute in water results an energetic cost due to the disruption of the hydrogen bond network in water for larger solutes.[6] When the hydrophobic unit is small, it can often be accommodated into the spontaneous cavities present in water[8] with some reorganization of the hydrogen bond network. A molecular level understanding that supports this picture for a small solute has emerged from a number of studies.[7−16] Results from these studies for small length scale solutes provided useful information regarding solvation and stability of dilute aqueous solutions of many hydrophobic molecules such as methane, rare gases, etc. However, direct use of these results to understand the nature of hydrophobicity at a larger length scale relevant to aggregation and association phenomena in biological systems has been difficult. Therefore, to understand various aggregation and association phenomena as diverse as protein folding, and self-assembly of hydrophobic nanomaterials, a thorough understanding of hydrophobicity at a larger length scale, although far from macroscopic, is essential.

A variety of physically appealing arguments have been used to explain such aggregation phenomena involving hydrophobic macromolecules. Persistence of the complete hydrogen bond network of contact water near a large or extended hydrophobic solute surface is geometrically impossible by mere rearrangement of the water molecules. Thus some have proposed that the resulting energetic imbalance can induce drying near such surfaces leading to the formation of a thin vapor layer[6,17] around the solute. In such a picture, when two such water-depleted large hydrophobic units come close to each other, number fluctuations near the interfaces lead to expulsion of the remaining water molecules from the inter solute region and induce collapse of the solute units. Various theoretical[6,18−20] and simulation[21−25] studies using an idealized model of the solute have supported the water expulsion mechanism for the hydrophobic association. However, a number of recent studies[26−33] using more realistic models for the solute have contradicted the idea of dewetting-induced collapse of large hydrophobic groups. Studies of stability of water inside a carbon nanotube,[26] between two nanoscopic hydrophobic surfaces,[30,31] and wetting of large methane clusters by water[29] showed solvent participation in the HI without dewetting. The evidence from simulations of a stable one-dimensional chain of water molecules inside a carbon nanotube[26] and that of a two-dimensional monolayer of water[30] between two nanoscopic planar hydrophobic solutes contradict the idea that energetic cost of some local disruption in the hydrogen bond network induces drying in or near a hydrophobic environment. Even a cluster of a few water molecules has been shown[27] to be stable in a spherical hydrophobic cavity.

One of the compensating effects to the energetic cost due to minor disruption of hydrogen bond of water appears to come from the solute−solvent attractive dispersion interactions. In a series of recent studies,[30,32,34,35] the importance of attractive solute−solvent interaction on the wetting/dewetting behavior of nanoscopically large solutes has been clearly demonstrated. It has been explicitly shown[30−32] that the cumulative effect of a large number of small solute−solvent attractive interactions can change large solute hydration behavior. In particular, the mechanism of the contact pair formation for a purely repulsive model nanoscopic solute in water has been shown[30] to be completely different from that for a system with reasonable dispersion interactions. The importance of an attractive interac-

* Corresponding author. Fax: (713) 743-2709. E-mail: pettitt@uh.edu.
† Present address: Theoretical Chemistry Section, Chemistry Group, Bhabha Atomic Research Centre, Mumbai 400 085, India.

10.1021/jp056909r CCC: $33.50
Published on Web 04/04/2006

tion between solute and the solvent on the hydration and domain collapse of proteins has also been demonstrated[28] recently.

Solutes in water at ambient conditions can change the vapor−liquid phase boundary. In particular, location of the vapor−liquid phase boundary in the vicinity of a large nanoscopic hydrophobic solute is highly dependent[35] on the extent of solute−water attractive interactions. Molecular level understanding of hydrophobicity at this length scale is thus far from being complete.[36]

A large increase in heat capacity when a hydrophobic solute is solvated in water is a defining thermodynamic signature of hydrophobic interaction. Understanding the thermodynamics of nonpolar solvation[37] is thus central to the understanding of the hydrophobic interaction. Relative contributions of entropy and enthalpy to the free energy of association determine the thermodynamic driving force of hydrophobicity-induced aggregation. For small hydrophobic solutes in water, it is well established that nonpolar solvation in water near room temperature is dominated by favorable entropic contribution. A large number of simulation studies of methane association in water have shown[12,14−16] the contact pair state to be entropically stabilized. As has been already mentioned, extrapolation and generalization of these small length scale results to understand aggregation phenomena of large biomacromolecules may not be straightforward, because of the multifaceted nature of hydrophobic hydration. It has been proposed[48] and recently demonstrated,[49] based on the hydration behavior of a purely repulsive model hydrophobic solute, that hydration thermodynamics changes from entropic for small solutes to enthalpic for large solutes. As has been shown earlier, inclusion of small van der Waals attractions between solute atoms and water changes the mechanism of association for nanoscopic solutes from that of its purely repulsive analogue.[30] It is therefore important to investigate whether thermodynamics of association of more realistic solutes with slowly varying weakly attractive dispersion interactions (in addition to the usual repulsive interaction) follows the same thermodynamic crossover as observed in case of hard sphere solutes.

In our previous work, we have calculated the free energy as function of separation, commonly known as the potential of mean force (PMF), between two nanoscopic hydrophobic solutes in explicit water. The PMF was obtained from molecular dynamics sampling in the isothermal−isobaric (NPT) ensemble in combination with free energy perturbation (FEP) methodology.[30,38,39] In the present work, we decompose the PMF into entropic and enthalpic contributions and investigate the mechanistic implications.

II. Methods

We have used computer simulation to study the thermodynamic behavior of the hydrophobic interaction between two nanoscopic, hydrophobic, planar solutes in water. The entropy of association has been calculated from the temperature derivative of the PMF via finite differences.[50]

We label solutes, u, and solvent, v. The solvent water molecules were modeled by the three-site SPC/E[40] model. Each of the hydrophobic solutes considered here was modeled as a graphite-like sheet or plate made up of sp^2 carbon atoms placed in a flat, hexagonal lattice with carbon−carbon bond lengths of 1.4 Å with force field parameters from the AMBER force field.[41] Each of the solute plates for our study has 60 carbon atoms with dimensions of ∼11 Å × 12 Å between nuclear centers or around 15 Å total van der Waals diameter.

Entropy is calculated from the finite difference temperature derivative of the PMF or $\Delta G(r)$ at each inter solute separation r, viz.,

$$-S(r) = \frac{\Delta G(r, T + \Delta T) - \Delta G(r, T)}{\Delta T} \tag{1}$$

In the present calculation, values of T and ΔT are chosen to be 298 and 20 K, respectively. The enthalpy contribution to the free energy, $\Delta H(r)$, can be obtained from entropy $S(r)$ and the PMF $\Delta G(r)$ at temperature T.

$$\Delta H(r) = \Delta G(r) + T\,\Delta S(r) \tag{2}$$

To elucidate the contribution from solvent molecules to the PMF we evaluate the solvent contribution $\Delta W_v(r)$ to the PMF $\Delta G(r)$ by subtracting the direct potential between two solutes, $U_{uu}(r)$ from the PMF, i.e.:

$$\Delta W_v(r) = \Delta G(r) - U_{uu}(r) \tag{3}$$

Here $\Delta W_v(r)$ is the solvent-induced contribution to the adiabatic work surface. As a free energy, we may split this into enthalpic and entropic contribution. Since the potential is independent of temperature, we decompose the solvent contribution to the enthalpy of association as

$$\begin{aligned}\Delta H_v(r) &= \Delta H(r) - U_{uu}(r) \\ &= \Delta W_v(r) + T\,\Delta S(r)\end{aligned} \tag{4}$$

To clarify the role of the reorganization of water molecules around large hydrophobic solutes, further analysis of $\Delta H_v(r)$ is necessary. The solvent contribution to the enthalpy of association can be split[16] further into two terms namely, a solute−solvent direct interaction, ΔU_{uv}, which represents the potential energy of interaction of a pair of solute plates separated by a distance r with the surrounding water molecules relative to its value at $r = \infty$ and the remaining contributions $\Delta H_{rem}(r)$ that include mechanical pressure−volume work and changes in the solvent−solvent interaction in the presence of a pair of solute plates at distance r, i.e.,

$$\Delta H_v(r) = \Delta U_{uv}(r) + \Delta H_{rem}(r) \tag{5}$$

The solute−solvent contribution, $\Delta U_{uv}(r)$ can be averaged directly from the simulation runs; one can then easily get the remaining contribution, $\Delta H_{rem}(r)$ from the above equation.

Simulations in the isothermal isobaric (NPT) ensemble were carried out using the molecular dynamics (MD) extended system approach of Nose and Anderson.[42−44] Periodic boundary conditions were applied and electrostatic interactions were calculated using the Ewald method.[45] The bonds and angles between oxygen and hydrogen atoms of the water molecules were constrained by use of the RATTLE algorithm,[45,46] and the solutes were kept rigid. All the systems were simulated at a target pressure of 1 atm and at target temperatures of 298 and 318 K. The equations of motion were integrated using the velocity Verlet algorithm[45,47] with a 2 fs time step. The PMFs were calculated using a free energy perturbation (FEP) technique. Details of the procedure are described elsewhere.[30]

III. Results and Discussions

A. Decomposition of Potential of Mean Force into Enthalpic and Entropic Contributions. The potential of mean forces, $\Delta G(r)$, as a function of the separation r between the

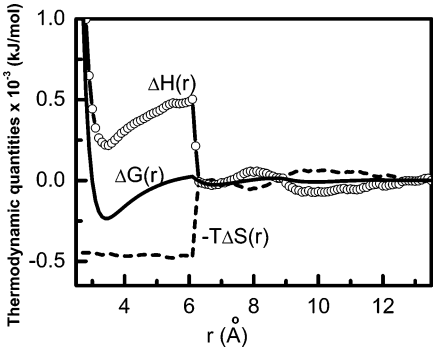

Figure 1. Enthalpic contribution, $\Delta H(r)$, (open circles with line) and entropic contribution, $-T\Delta S(r)$, (dashed line) to the potential of mean force, $\Delta G(r)$, (solid line) for a pair of planar nanoscopic nonpolar solutes in water at 298 K and 1 atm pressure.

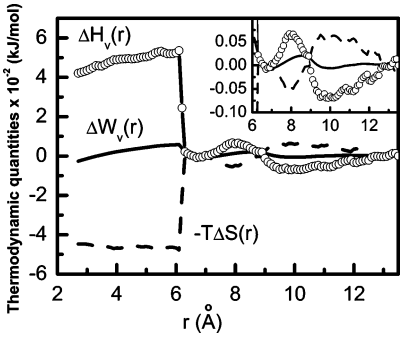

Figure 2. Solvent contribution, $\Delta W_v(r)$ to the PMF, $\Delta G(r)$ and its entropic ($-T\Delta S(r)$), and enthalpic ($\Delta H_v(r)$) contributions for the same system as in Figure 1. The keys are same as in Figure 1. In the inset the same plots are shown for intersolute separations of 6 Å and larger.

two large (60 atoms) parallel plates at normal pressure and two different temperatures have been calculated by the FEP technique using MD simulation for sampling. The entropic contribution, $-T\,\Delta S(r)$ to the PMF, $\Delta G(r)$, at 298 K is obtained through eq 1. The entropic ($-T\,\Delta S(r)$) and enthalpic ($\Delta H(r)$) contributions to the PMF at 298 K are shown in Figure 1 along with the PMF. The stabilizing effects of entropic and enthalpic contributions of the PMF act in opposite direction to each other, and the relative proportion of the two contributions depends on the inter solute distances. This is a form of the familiar macroscopic entropy−enthalpy compensation which has been seen for local quantities such as these reflected in a PMF for some time.[50]

The contact pair state is entirely stabilized by the favorable entropic contribution, enthalpic contribution being highly unfavorable. The favorable entropic contribution is so huge that it stabilizes the solute association even after compensating the unfavorable enthalpic effect. The entropic contribution at the contact state in the present case is around −460 kJ/mol. The entropy of association for a methane pair is around −4 kJ/mol,[13,16] which amounts to around −240 kJ/mol for 60 atom pairs, say those directly opposite to each other. The additional entropic stabilization thus arises from cross correlations in the solute−solute and solute−solvent contributions.

At lower interparticle separations, the enthalpic contribution is dominated by the steep repulsive part of the direct solute−solute potential $U_{uu}(r)$ and therefore change in the solvent contribution to enthalpy is masked. Eliminating the direct solute−solute potential part, $U_{uu}(r)$ from the PMF, we obtain the solvent contribution to the PMF, $\Delta W_v(r)$. Since the direct solute−solute interaction is independent of temperature, the solvent contribution to enthalpy, $\Delta H_v(r)$ can easily be obtained by subtracting the $U_{uu}(r)$ from the enthalpy term. The solvent contribution to the PMF is shown in Figure 2 along with its entropic ($-T\Delta S(r)$) and solvent-induced enthalpic ($\Delta H_v(r)$) contributions.

Stability of the first solvent separated state at an intersolute separation of around 7 Å is determined mostly by the stabilizing effect of the enthalpy, the entropic contribution at this separation being relatively small. However, the barrier between the contact pair state and first solvent separated state at around 6 Å is dominated by unfavorable enthalpy despite a considerable favorable contribution from the entropy. When the intersolute distance is shorter than 6 Å, a substantial increase in $\Delta H_v(r)$ and decrease in $-T\Delta S(r)$ are observed. We have shown earlier[30] that water forms a highly structured layer between the two solutes at an inter solute distance of 7.0 Å and it remains so down to around an intersolute distance of 6.0 Å. The large increase in entropy (decrease in $-T\Delta S(r)$ as shown in Figure 2) below 6 Å results from the release of the highly structured water from the intersolute region to the bulk. On the other hand, as a result of expulsion of water molecules from the intersolute region, an amount of favorable energy arising from attractive interactions between the solute and water in the confined region is lost. This results in a sharp increase in solvent-reflected enthalpy below an intersolute distance of 6 Å. A slight downward trend in the ΔH_v term from this point downward can be due either to an increase in favorable interactions between the water and the solute or to changes in water−water interactions. A decomposition of ΔH_v into solute−solvent and water−water interactions has, therefore, been performed and presented in the next subsection.

Beyond the first solvent-separated minimum in free energy we find another minimum at around an intersolute separation of 10 Å that corresponds[30] to the second solvent separated state with a solute−solvent configuration having two intervening water layers which is stabilized by enthalpy. The barrier between the first and the second solvent-separated minima is determined from a slight imbalance between the stabilizing enthalpic contribution and the destabilizing entropic contribution.

B. Contributions from Water−Water Interactions due to Solvent Reorganization around the Solute. With a change in intersolute distance, it is expected that water around the solute molecules will reorganize themselves, and therefore a change in water−water interaction should result. As mentioned earlier, quantification of this contribution due to change in water−water interaction to the solvent induced enthalpy is possible[16] if the direct solute water interaction can be calculated from the simulation trajectory. In the present study, we have calculated, from the configurations obtained from the MD trajectory, the interaction between the water and the pair of solute plates at various interparticle distances. The variation of this term with respect to its value at a large intersolute separation is designated here as $\Delta U_{uv}(r)$ and is shown in Figure 3. At large intersolute separation, $\Delta U_{uv}(r)$ is nearly zero and it deviates only slightly when the intersolute distance is reduced to 9 Å. On further reduction of the inter solute distance, the change in this contribution is noticeable. When the intersolute separation is further reduced below 6 Å, $\Delta U_{uv}(r)$ becomes highly unfavorable, essentially constant, and contributes significantly to the unfavorable ΔH_v term. The drop in interaction energy between the solute and confined water when the intersolute separation is reduced from say 6.2 Å, where a monolayer of water exists in the confined region, to 5.8 Å, where no water molecules are sterically allowed in the intersolute region, is around 150 kJ/mol (see Table 1 of ref 30). This is almost the same as the increase in $\Delta U_{uv}(r)$ at this point, as shown in Figure 3. Thus,

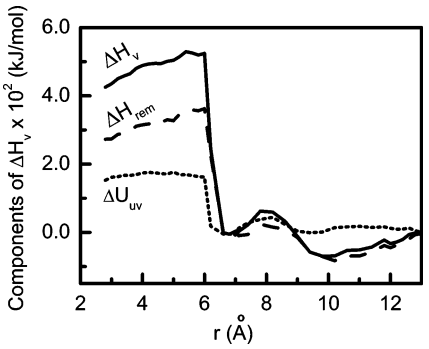

Figure 3. Solvent-induced contribution to enthalpy of association, $\Delta H_v(r)$ (solid line) is split into the change in energy of interaction of the solute pair with water molecules, $\Delta U_{uv}(r)$, (dotted line) and the remaining contributions from the change in water−water interactions and other mechanical work, $\Delta H_{rem}(r)$, (dashed line). In this plot all quantities are referenced to the solute pair at 13 Å.

the increase in $\Delta U_{uv}(r)$ at this point originates solely from the reduction in favorable interactions of the confined water with the solute plates due to expulsion of water from between the two solute plates.

When the contribution due to direct solute−solvent interactions, $\Delta U_{uv}(r)$ is subtracted from the solvent contribution to the enthalpy ($\Delta H_v(r)$), one obtains the remaining contributions ($\Delta H_{rem}(r)$) arising from the change in water−water interactions around the solute plates and from the pressure−volume work, $P\Delta V$. At 1 atm pressure, the $P\Delta V$ term is small and the behavior of ΔH_{rem} is mainly dictated by the contributions from the changes in interactions. It is important to observe that the contribution from the $\Delta H_{rem}(r)$ term is substantial in the $\Delta H_v(r)$ throughout the entire range of interparticle separations considered here. As already shown, near the contact pair state a significant unfavorable contribution in $\Delta H_v(r)$ comes from the direct solute−water interaction part, $\Delta U_{uv}(r)$, which accounts for more than 30% of the increase in the solvent induced enthalpy change. However, an unfavorable contribution also arises from the change in the interactions represented by ΔH_{rem}. When all the water molecules are expelled from the intersolute region into the bulk, a reorganization is required to accommodate these expelled water molecules and so some less favorable interactions of the water molecules may result. The nature and amount of decrease in $\Delta H_v(r)$ in the region of inter solute separations of 6 Å to 3 Å is entirely due to the similar change in the ΔH_{rem} term.

IV. Conclusions

We have investigated the detailed thermodynamics of nanoscopically large hydrophobic solute plates modeled as graphene sheets in explicit water. The entropic and enthalpic contributions to the PMF were calculated from the temperature dependence of the PMF obtained from the MD simulation in conjunction with FEP techniques. Here we mainly confirm an old theoretical picture of the hydrophobic interaction. In particular we find that contact (solvent excluding) configurations are entropically stabilized. Solvent-separated configurations are enthalpically stabilized or show entropy−enthalpy compensation or cancellation.

The stabilization of the contact pair state is mainly due to an increase in entropy arising from the expulsion of the highly structured water layer from the intersolute region. It is, however, important to note that the expulsion of water between the plates occurs only due to steric constraints. The highly unfavorable solvent-induced contribution to the enthalpy change at the contact pair state arises from the changes in water−water interactions. The PMF at the first solvation barrier is dominated by unfavorable enthalpic contributions as compared to the stabilizing entropic term.

The results presented here clearly demonstrate the relative roles of entropy and enthalpy in stabilizing various solute−solvent configurations of nanoscopic hydrophobic solutes in water at ambient conditions. We have shown that thermodynamic behavior of association of solutes with realistic interactions in water does not show any crossover[48] from entropic to enthalpic behavior in this solute size range, which is similar to that expected for many biomolecular assemblies. To better understand the association of large hydrophobic solutes in water and its relation to the aggregation phenomena observed in biological systems, future studies will include the effects of pressure, salt concentrations, and denaturant on the PMF as well as on the relative contributions of entropy and enthalpy to the PMF.

Acknowledgment. We gratefully acknowledge NIH, the R.A. Welch foundation, and TiiMES, funded by NASA Cooperative Agreement No. NCC-1-02038, for partial financial support of this work. The computations were performed in part using the NSF meta center facilities and the Molecular Science Computing Facility in the W.R. Wiley Environmental Molecular Sciences Laboratory, a national scientific user facility sponsored by the DOE's Office of Biological and Environmental Research and located at Pacific Northwest National Laboratory, operated for the DOE by Battelle.

References and Notes

(1) Kauzmann, W. *Adv. Protein Chem.* **1959**, *14*, 1.
(2) Pratt, L. R.; Pohorille, A. *Chem. Rev.* **2002**, *102*, 2671.
(3) Tanford, C. *The Hydrophobic Effect: Formation of Micelles and Biological Membranes*; John Weiley: New York, 1973.
(4) Dill, K. A. *Biochemistry* **1990**, *29*, 7133.
(5) Ludemann, S.; Schreiber, H.; Abseher, R.; Steinhauser, O. *J. Chem. Phys.* **1996**, *104*, 286.
(6) Lum, K.; Chandler, D.; Weeks, J. D. *J. Phys. Chem. B* **1999**, *103*, 4570.
(7) Pangali, C.; Rao, M.; Berne, B. J. *J. Chem. Phys.* **1979**, *71*, 2975.
(8) Hummer, G.; Garde, S.; Garcia, A. E.; Pohorille, A.; Pratt, L. R. *Proc. Natl. Acad. Sci. U.S.A.* **1996**, *93*, 8951.
(9) Perkyns, J. S.; Pettitt, B. M. *J. Phys. Chem.* **1996**, *100*, 1323−1329.
(10) Hummer, G.; Garde, S. *Phys. Rev. Lett.* **1998**, *80*, 4193.
(11) Smith, D. E.; Haymet, A. D. J. *J. Chem. Phys.* **1993**, *98*, 6445.
(12) Smith, D. E.; Zhang, L.; Haymet, A. D. J. *J. Am. Chem. Soc.* **1992**, *114*, 5875.
(13) Shimizu, S.; Chan, H. S. *J. Am. Chem. Soc.* **2001**, *123*, 2083.
(14) Rick, S. W.; Berne, B. J. *J. Phys. Chem.* **1997**, *101*, 10488.
(15) Rick, S. W. *J. Phys. Chem. B* **2000**, *104*, 6884.
(16) Ghosh, T.; Garcia, A. E.; Garde, S. *J. Chem. Phys.* **2002**, *116*, 2480.
(17) Stillinger, *J. Solution Chem.* **1973**, *2*, 141.
(18) Huang, D. M.; Chandler, D. *Proc. Natl. Acad. Sci. U.S.A.* **2000**, *97*, 8324.
(19) Huang, D. M.; Geissler, P. L.; Chandler, D. *J. Phys. Chem. B* **2001**, *105*, 6704.
(20) Huang, D. M.; Chandler, D. *J. Phys. Chem. B* **2002**, *106*, 2047.
(21) Berard, D. R.; Attard, P.; Patey, G. N. *J. Chem. Phys.* **1993**, *98*, 7236.
(22) Wallqvist, A. Berne, B. J. *J. Phys. Chem.* **1995**, *99*, 2885.
(23) Wallqvist, A. Berne, B. J. *J. Phys. Chem.* **1995**, *99*, 2893.
(24) Huang, X.; Margulis, C. J.; Berne, B. J. *Proc. Natl. Acad. Sci. U.S.A.* **2003**, *100*, 11953.
(25) Walqvist, A.; Gallicchio, E.; Levy, R. M. *J. Phys. Chem.* **2001**, *105*, 6745−6753.
(26) Hummer, G.; Rasaiah, J. C.; Noworyta, J. P. *Nature* **2001**, *414*, 188. Sansom, M. S. P.; Biggin, P. C. *Nature* **2001**, *414*, 156.
(27) Waghe A.; Rasaiah, J. C.; Noworyta, J. P.; Hummer, G. *J. Chem. Phys.* **2002**, *117*, 10789.
(28) Zhou, R.; Huang, X.; Margulis, C. J.; Berne, B. J. *Science*, **2004**, *305*, 1605.

(29) Ashbaugh, H. S.; Paulaitis M. E. *J. Am. Chem. Soc.* **2001**, *123*, 10721−10728.
(30) Choudhury, N.; Pettitt B. M. *J. Am. Chem. Soc.* **2005**, *127*, 3556.
(31) Choudhury, N.; Pettitt B. M. *J. Phys. Chem. B* **2005**, *109*, 6422.
(32) Choudhury, N.; Pettitt B. M. *Mol. Sim.* **2005**, *31*, 457.
(33) Subramanian, V.; Yin, H.; Rasaiah, J. C.; Hummer, G. *Proc. Natl. Acad. Sci. U.S.A.* **2004**, *101*, 17002.
(34) Choudhury, N.; Pettitt B. M. Special Volume of the Royal Society of Chemistry entitled *Modeling Molecular Structure and Reactivity in Biological Systems*; Naidoo, K. J., Hann, M., Gao, J., Field, M., and Brady, J., Eds.; (communicated).
(35) Choudhury, N.; Pettitt B. M. *Proc. Nat. Acad. Sci.* (Communicated).
(36) Ball, P. *Nature* **2003**, *423*, 25.
(37) Ben-Neim, A. In *Hydrophobic Interactions*; Plenum Press: New York, 1980.
(38) Zwanzig, R. W. *J. Chem. Phys.* **1954**, *22*, 1420.
(39) Linse, P. *J. Am. Chem. Soc.* **1993**, *115*, 8793.
(40) Berendsen, H. J. C.; Grigera, J. R.; Straatsma, T. P. *J. Phys. Chem. B* **1987**, *91*, 6269.
(41) Cornell, D. W.; Cornell, W. D.; Cieplak, P.; Bayly, C. I.; Gould, I. R.; Merz, K. M.; Ferguson, D. M.; Spellmeyer, D. C.; Fox, T.; Caldwell, J. W.; Kollman, P. A. *J. Am. Chem. Soc.* **1995**, *117*, 5179.
(42) Nose, S. *Mol. Phys.* **2002**, *100*, 191.
(43) Andersen, H. C. *J. Chem. Phys.* **1980**, *72*, 2 384.
(44) Nose, S.; Klein, M. L. *Mol. Phys.* **1983**, *50*, 1055.
(45) Allen, M. P.; Tildesley, D. J. *Computer Simulation of Liquids*; Oxford University, New York, 1987.
(46) Andersen, H. C. *J. Comput. Phys.* **1983**, *52*, 24.
(47) Swope, W. C.; Andersen, H. C.; Berens, P. H.; Wilson, K. R. *J. Chem. Phys.* **1982**, *76*, 637.
(48) Chandler, D. *Nature* **2005**, *437*, 640.
(49) Rajamani S.; Truskett, T. M.; Garde S. *Proc. Natl. Acad. Sci. U.S.A.* **2005**, *102*, 9475.
(50) Pettitt, B. M.; Rossky, P. J. *J. Chem. Phys.* **1986**, *84*, 5836.